

Differential diffusion: an oceanographic primer

Ann Gargett

Institute of Ocean Sciences, Patricia Bay

P.O. Box 6000

Sidney, B.C.

V8L 4B2 CANADA

accepted, Progress in Oceanography

June, 2001

Abstract: Even where mean gradients of temperature T and salinity S are both stabilizing, it is possible for the larger molecular diffusivity of T to result in *differential diffusion*, the preferential transfer of T relative to S . The present note reviews existing evidence of differential diffusion as provided by laboratory experiments, numerical simulations, and oceanic observations. Given potentially serious implications for proper interpretation of estimates of diapycnal density diffusivity from both ocean microscale measurements and ocean tracer release experiments, as well as the notable sensitivity of predictive global ocean models to this diffusive parameter, it is essential that this process be better understood in the oceanographic context.

1. Introduction:

Diapycnal mixing of density occurs at spatial scales which are unresolved in even regional-scale numerical models of the ocean. Moreover, the models of large-scale ocean circulation presently being used to predict evolution of the earth's climate system have proven to be very sensitive to the magnitude of the parameter normally used to describe the effects of diapycnal mixing at sub-grid scales (Bryan 1987). It is thus essential to have parameterizations of the effects of small-scale mixing which are not only accurate as far as magnitude in the present ocean, but also include an understanding of the underlying causative physical processes, since these may alter under climate-induced changes in mean ocean properties.

In the ocean, diapycnal mixing of density is actually a process of mixing two variables, heat (or temperature T) and salt (or salinity S), which both contribute to the density of ocean water. All numerical ocean models presently parameterize unresolved interior diapycnal fluxes as a turbulent diffusivity K times a mean property gradient normal to isopycnals. Most models also use $K = K_T = K_S$, i.e. the same diffusivities for T and S . There are, however, small-scale processes which transport T and S differentially. The best-known are the double-diffusive processes (salt fingering and double-diffusive layering) which occur in ocean regions where

mean T and S gradients have opposite influence on density, and which are the declared focus of SCOR WG108. Almost unacknowledged by the oceanic community is the fact that even when both T and S gradients are stabilizing, there is potential for differential transport of T and S in the ocean (Gargett 1988: 1997).

Under certain conditions, it is possible for the larger molecular diffusivity of T to produce preferential turbulent transfer of T relative to S. The mechanism by which this occurs is similar to that underlying double diffusion: a major difference is that the kinetic energy which drives double diffusion is supplied by the release of potential energy from the gravitationally unstable component of the mean fields, while in differential diffusion, kinetic energy comes from “ordinary” turbulence. In this latter case, the conceptual picture is that of a locally overturning eddy which stirs an embedded scalar field. The amount of scalar variance which is dissipated within the eddy decay time scale τ_e is influenced by the turbulent Reynolds number $Re = u\ell/\nu$ (where u and ℓ are characteristic turbulent velocity and length scales and ν is the fluid kinematic viscosity), since this determines the range of scales present in the flow, hence the time required to stir down to the Kolmogorov scale. In addition, the dissipated variance may also depend upon scalar Schmidt number $Sc = \nu/D$ (where D is the scalar molecular diffusivity) which sets the additional time needed to strain the scalar to its own dissipation scale, ie the scale at which the scalar finally mixes irreversibly. For very diffusive scalars (small Sc), scalar variance can be entirely erased within the decay time scale of the velocity field, while effectively non-diffusive scalars (very high Sc) will experience almost no transfer of variance to their much smaller diffusive scales within the same period of time. Since irreversible scalar mixing is rooted in the elimination of scalar variance by intermingling at a molecular level, these differences can result in *differential diffusion* of scalars, such as T and S in seawater, which have very different molecular diffusivities.

Because differential diffusion arises through the same differences in molecular diffusivities which lead to double diffusion, the members of SCOR WG 108 considered it reasonable to include in its report a summary of the state of our knowledge of this lesser known process, as well as of the more familiar double diffusive processes. This paper thus reviews existing evidence of differential diffusion as provided by laboratory experiments (Section 2), numerical simulations (Section 3), and oceanic observations (Section 4). Section 5 considers the question of necessary conditions for significant differential diffusion, as well as potential implications of the existence of this process for interpretation of both ocean microscale measurements and ocean tracer release experiments.

2. Laboratory evidence of differential diffusion

Turner (1968) first demonstrated differential diffusion in separate laboratory experiments, using T and S in turn to produce a two-layer density stratification which was subsequently mixed away by grid-generated turbulence. As seen in Figure 1 (from Turner 1973), at high values of a Richardson number $Ri_0 \equiv g(\Delta\rho/\rho)\ell_1/u_1^2$ defined in terms of turbulent velocity and length scales u_1 and ℓ_1 , the effective transport of density produced by T was consistently higher than that occurring when the same density difference $\Delta\rho$ was produced by S.

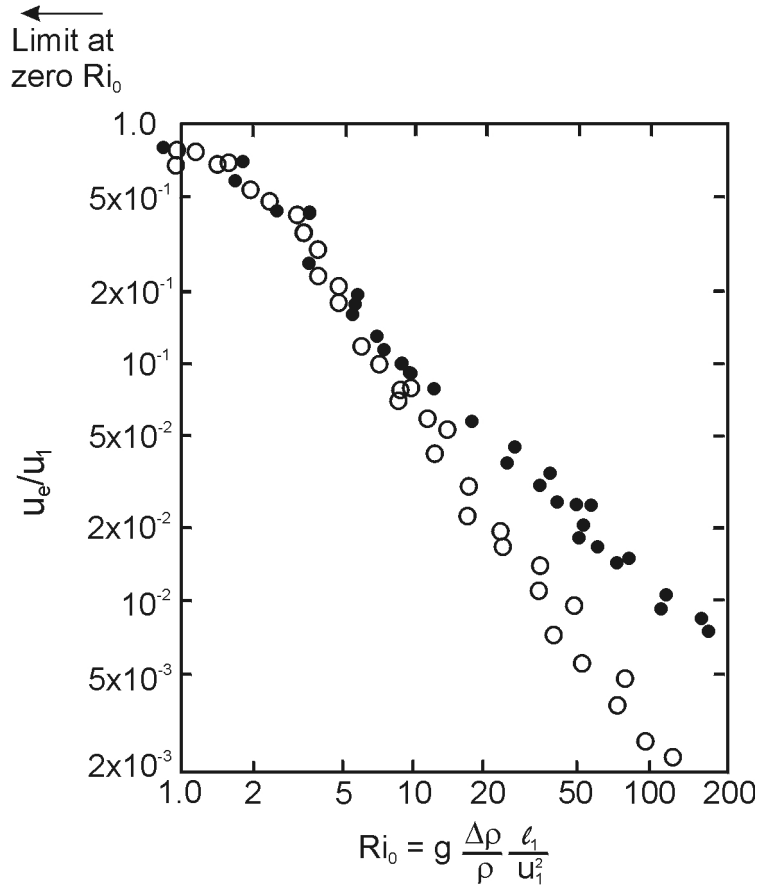


Figure 1: From Turner (1973): comparison between directly measured entrainment (mixing) velocity associated with grid-stirring on one side of a density interface produced respectively by (filled circles) temperature and (open circles) salt. The dimensionless mixing rates obtained by Turner (1968) are plotted here against a Richardson number Ri_0 calculated with turbulent length ℓ_1 and velocity u_1 scales characteristic of the grid turbulence.

Altman and Gargett (1990) subsequently demonstrated similar effects in two-layer grid-stirring experiments where T and S made simultaneous contributions to the initial density step. Figure 2 illustrates the evolution (right to left) of density entrainment rate (triangles) over the course of a typical run-down experiment, plotted against the same Ri_0 defined by Turner (1973). Calculated entrainment rates for T and S individually obey power laws which were unchanged by the presence of the second stratifying component. While the initial density entrainment rate was roughly that of T when present alone (circles), it approached that of S alone (crosses) by

the end of the run, when the initial T-contrast had disappeared but salt stratification remained. While these experiments confirmed the action of differential diffusion in the two-component system, they exhibited some unsatisfactory features. Despite an effort to duplicate the laboratory set-up of Turner's (1968) experiments, absolute entrainment rates differed substantially, suggesting large sensitivity to small details of the geometry of the apparatus. In addition, there was an unexplained (although small) increase in entrainment magnitudes of the individual species in the two-component runs relative to the single-component experiments. These and other difficulties have made determination of appropriate entrainment law(s) for such "mixing box" experiments the subject of continuing debate (Fernando 1991).

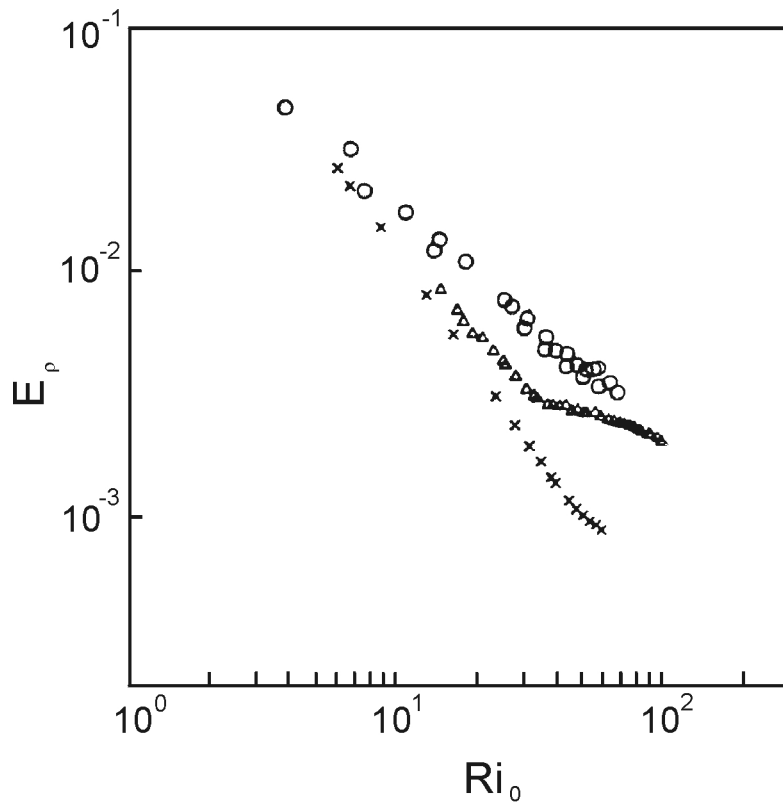


Figure 2: From Altman and Gargett (1990). (a) Entrainment rate as a function of Richardson number Ri_0 , for grid-stirring on both sides of a density interface produced by temperature alone (open circles), salt alone (crosses), and both temperature and salt (triangles) present simultaneously. Rundown experiments proceed from right to left. In the simultaneously T- and S-stratified run, density entrainment first follows the T-entrainment curve, but finally tends towards the S-entrainment curve as the initial contrast in T is mixed away more rapidly than the initial S-contrast.

Acceptance of potential oceanic importance of the results of such experiments has been hindered by the fact that both the stratification (two-layer) and the turbulence generation mechanism (grid oscillation) are “non-oceanic”. However a broader literature on differential diffusion has been accumulating, originating in the interest of the engineering community in turbulent diffusion flames (also known as nonpremixed flames), in which gaseous fuels and oxidants are initially separated and combustion occurs only when mixing is complete to the molecular scale within at least some fraction of the volume. Bilger (1989) reviewed existing evidence suggesting strong Schmidt-number effects on mixing interface structure and entrainment in both gaseous and liquid reactive jet flows. Since then, measurements of differential diffusion have been reported in a variety of nonreacting jets, characterized by a wide range of jet Reynolds number and using both active (Kerstein 1990; Smith et al. 1995) and passive (Saylor and Sreenivasan 1998) scalars. Komori and Nagata (1996) have recently demonstrated effects of molecular diffusivity on scalar transport in strongly stratified water flows downstream of turbulence-generating grids. In unsheared flows, differential transport of T and S became evident near the time when counter-gradient fluxes first developed, roughly $Nt = 2$, where $N = (-g \rho_0^{-1} \rho_z)^{1/2}$ is the Brunt-Vaisala frequency. While the addition of mean shear decreased the observed differential fluxes, cumulative differences in T and S transports are still evident even at Ri as low as ~ 0.4 , as well as at the value $Ri \sim O(1)$ believed typical of the stratified interior of the ocean (cf. Fig. 22 of Komori and Nagata 1996). In contrast, Rehmann (1995) reports the absence of measurable differential diffusion of T and S in laboratory experiments where turbulence was generated by dragging a grid through a quiescent stratified fluid. Rehmann (1995) notes however that experimental constraints made it impossible to set the Reynolds number $Re_M = UM/\nu$ and the Richardson number $Ri_M = (NM/U)^2$, defined in terms of grid spacing M and mean flow speed U , independently of the Schmidt number, so changes due to variation in Sc may have been masked by changes in Re in these experiments.

In summary, there is ample laboratory evidence for the existence of the process of differential diffusion in a variety of gas and liquid flows, often even at what are considered to be high Reynolds numbers (Broadwell and Mungal 1991).

3. Numerical modelling of differential diffusion

Differential diffusion has been modelled by a linear-eddy technique (Kerstein 1990), as well as by direct numerical simulation (DNS) of passive (Yeung and Pope 1993) and active (Merryfield et al. 1998) scalars.

Kerstein (1988) developed a novel modelling technique which resolves all relevant physical scales for Re up to $O(10^4)$, at the price of sacrificing the three-dimensionality of turbulent flows. The stirring effect of turbulent eddies on a scalar field is simulated by a one-dimensional stochastic rearrangement process. Coupled with deterministic treatment of molecular diffusion according to Fick's law, this linear-eddy model has been successful in capturing many features of mixing in a variety of laboratory flows. Kerstein (1990) modified the original model for application to mixing in round jets, and predicted significant differential diffusion of H_2 and propane at $Re_{jet} = 5000$, but not at $Re_{jet} = 20000$. These predictions are in qualitative agreement with measurements by Bilger and Dibble (1982), although quantitative discrepancies exist.

An alternate computational strategy for investigating differential diffusion is to resolve the dissipation scales of the relevant scalars directly in simulations of three-dimensional turbulence. With this "brute-strength" approach, computational limitations impose compromises on either or both of the ranges of Re and Sc which can be addressed. Being motivated by laboratory diffusion flames, Yeung and Pope (1993) considered only scalars with $Sc \leq 1$, thus dramatically reducing spatial resolution requirements relative to calculations with $Sc \gg 1$, and allowing their 64^3 calculation to achieve a Taylor scale Reynolds number of $Re_\lambda = 38$. In order

to treat the oceanographically relevant case of the active scalars T and S which determine the density of seawater, and for which Prandtl number $Sc_T = Pr = 7$ and $Sc_S = 700$, Merryfield et al. (1998) reduced the dimension of calculation to two. As seen in Figure 3, their two-dimensional simulations were able to achieve ranges of initial Reynolds number $10 \leq Re \leq 160$ and Froude number $0.15 \leq Fr \leq 110$ ($Re = u \ell / \nu$ and $Fr = u / N \ell$, where N is the Brunt-Vaisala frequency and u and ℓ are velocity and length scales characteristic of the field of turbulent kinetic energy which

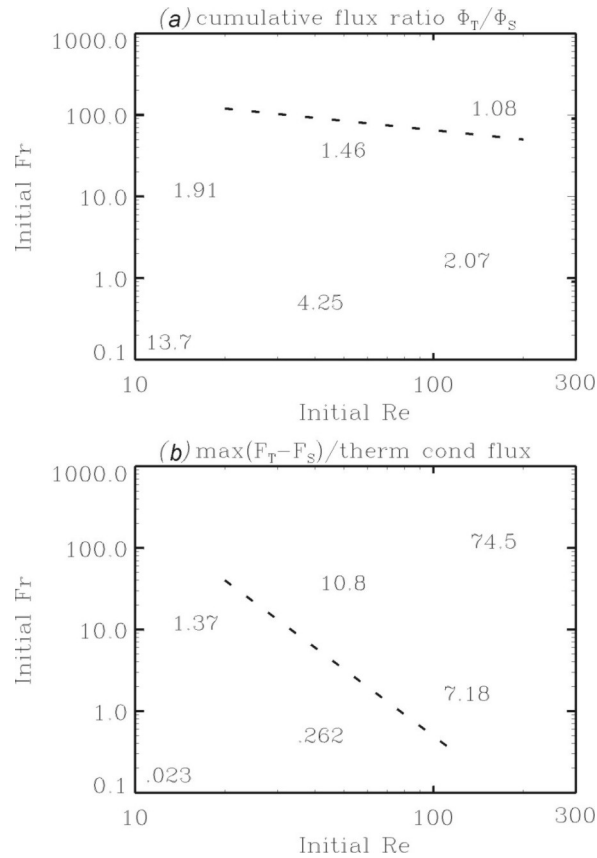


Figure 3: From Merryfield et al. (1998). Results of direct numerical simulation of T and S mixing by two-dimensional turbulence, displayed in the space of $\{Re, Fr\}$ calculated from initial turbulence properties. (a) Ratio of cumulative T-flux (Φ_T) to cumulative S-flux (Φ_S). The dashed line schematically divides the region of unequal cumulative fluxes ($\Phi_T/\Phi_S > 1$, below the line) from that with $\Phi_T/\Phi_S \approx 1$. (b) Maximum instantaneous flux difference $F_T - F_S$, in units of thermal conductive flux. Above the dashed line, $F_T - F_S$ exceeds roughly twice the thermal conductive flux. These results suggest that differential diffusion is important (fluxes greater than twice molecular, with cumulative flux ratios greater than 1) in the parameter range roughly between the two dashed lines.

was supplied at $t=0$ and subsequently decayed). The simulations revealed a sizeable region of $\{Re, Fr\}$ space (below the dashed line in Fig.3a and above that in Fig.3b) in which the ratio of cumulative T- to S-flux was greater than 1, indicating preferential diffusion of T, while at the same time the T-flux magnitude was significantly larger than that caused by molecular diffusivity, indicating the action of turbulence, however weak. While suggestive, results from two-dimensional calculations are vulnerable to the criticism that two-dimensional turbulence has energy cascade properties which differ from those of three-dimensional turbulence, hence may not be applicable to the latter. Fully three-dimensional simulations are now being undertaken in order to confirm the 2-D results and to compare numerically achievable values of Re and Fr to values typical of the stably stratified ocean interior where turbulence (as revealed by those oceanic variables such as temperature dissipation rate χ_T and kinetic energy dissipation rate ϵ which we are routinely able to measure) appears to be weak and sporadic.

4. Observational evidence of differential diffusion?

Direct observational evidence for the operation of differential diffusion in the ocean is sparse and as yet inconclusive. Figure 4 shows free-fall CTD casts taken during the course of increasing ebb flow in a B.C. tidal channel (Gargett, unpublished data). The observed nonlinear evolution (B, C) of the initially linear T/S curve (A), could not result from vertical mixing with equal T and S diffusivities, but would arise if T were mixed more efficiently than S. However potential effects of horizontal processes have not yet been ruled out in this case.

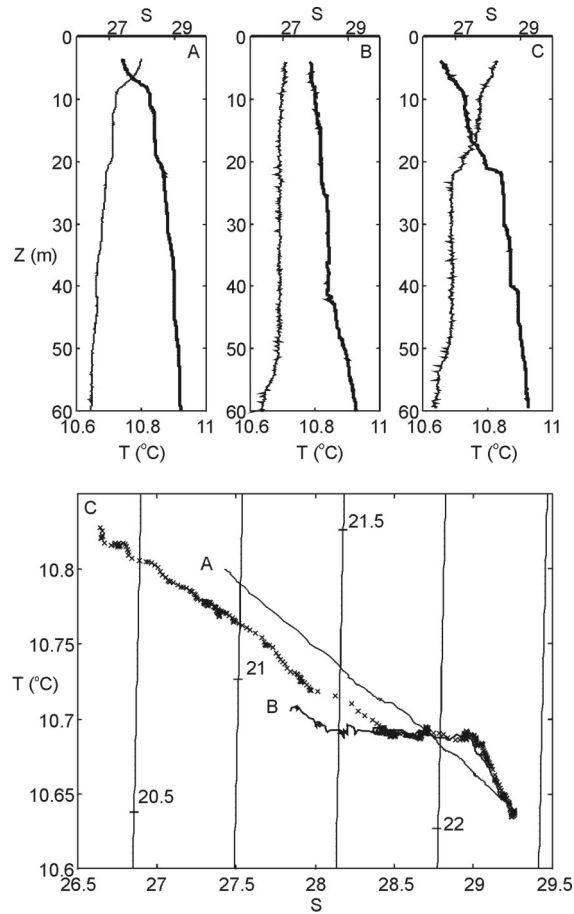


Figure 4: The upper panels show free-fall CTD profiles of T (light lines) and S (heavy lines) taken from an anchored ship at (A) high water slack tide, and (B, C) as an ebb tidal flow increased over the subsequent three hours. Ordinary turbulent mixing of the water column in (A) would retain the original linear relation shown in the T/S plot below, merely decreasing the range of T and S. Instead, the turbulence (revealed variously by large density overturning scales, critical mean shears and large vertical velocities, not shown here) results in a strongly nonlinear deformation of the T/S relation. The observed change in the T/S relation is in the sense that would be associated with differential diffusion, ie $K_T > K_S$, though other explanations cannot be discounted at present.

Even should it prove possible to do so, the observational situation, in which density is determined almost entirely by S and T acts effectively as a passive scalar, is quite different from that simulated by Merryfield et al. (1998), where T and S made equal contributions to the density stratification. Although the engineering literature shows that differential diffusion acts on passive as well as active scalars, the mechanisms, hence the magnitude of effects, are likely

to vary according to whether or not the scalar field substantially affects the dynamics of the turbulence (see discussion below of conceptual models). This suggests the need to investigate potential effects on differential diffusion of $R_p = \alpha T_z / \beta S_z$, the ratio which describes the relative contributions of T and S to the density stratification (assuming a linear equation of state).

More convincing evidence of the action of differential diffusion may be the interleaving T/S structures observed in what Rudels et al. (1994) term Upper Polar Deep Water, doubly-stable regions of the Arctic water column between about 700 and 1000m (Figure 5). Making the necessary modifications to the Walsh and Ruddick (1995) theory for intrusions driven by double-diffusion, Merryfield (2001) uses linear stability analysis to determine values of K_T and K_S which are consistent with observed intrusion thicknesses in the range of 40-60m. While the required values of K_T lie within a range of $0.01 \text{ cm}^2\text{s}^{-1} \leq K_T \leq 0.03 \text{ cm}^2\text{s}^{-1}$, a factor of 3-10 smaller than values normally quoted for the interior of other oceans, the Arctic interior is recognized as a low turbulence environment (Padman and Dillon 1987). The necessary diffusivity ratio K_S/K_T lies in a range $0.6 \leq K_S/K_T \leq 0.7$ which is reasonable based on laboratory measurements (and nearly undetectable with present observational techniques). Predicted growth rates for the intrusions are also consistent with the appearance of measurable interleaving structures on time scales shorter than the estimated residence time of the Upper Polar Deep Water in the Arctic Ocean.

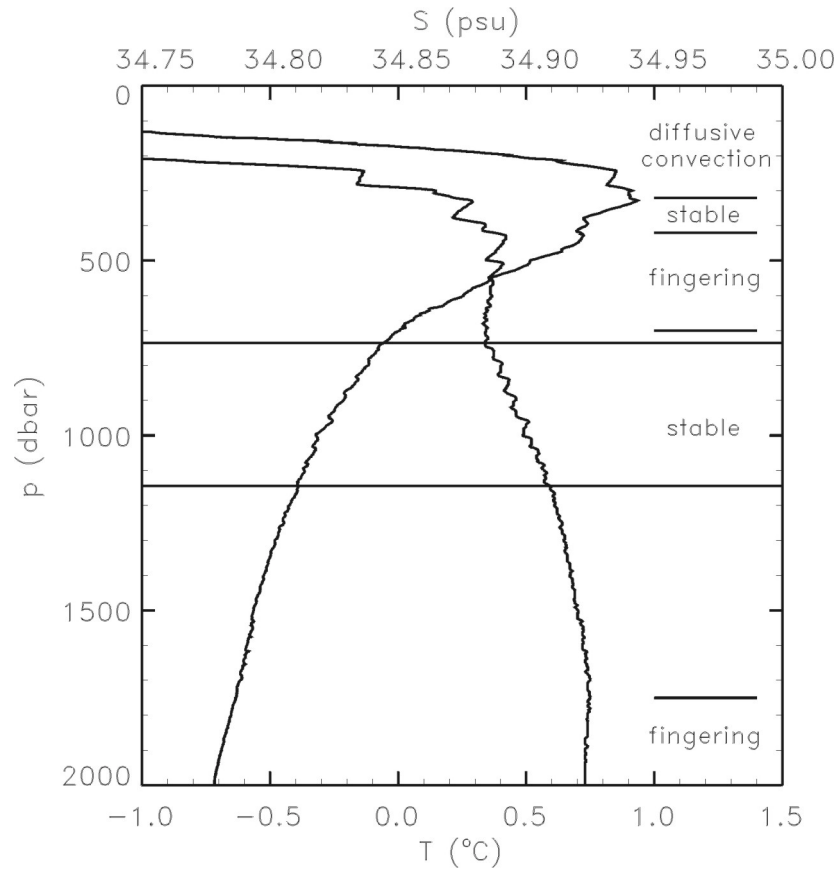


Figure 5: Temperature and salinity vs. depth at an Arctic Ocean station: from Merryfield (2001), data courtesy of Peter Jones, Bedford Institute of Oceanography. The horizontal lines bracket strong intrusive features between about 700 and 1100m, in doubly-stable Upper Polar Deep Water. Differential diffusion with $K_T > K_S$ is one possible explanation for the existence of intrusions in a part of the water column which is stable to double-diffusion.

Finally, Nash and Moum (2001) have very recently reported the first simultaneous measurements of both temperature and salinity variance dissipation rates, χ_T and χ_S respectively, using microprofiler data taken on the Oregon continental shelf. Estimates of irreversible temperature and salinity fluxes can be made from these dissipation rates, using the method of Osborn and Cox (1972). From such microscale fluxes, determined over four hundred independent turbulent patches, they found an average value of $K_S/K_T = \chi_S/\chi_T (dT/dS)^2 = 0.7 \pm 20\%$ for the ratio of haline to thermal turbulent diffusivities. Despite the fairly large error

bars on this (very difficult!) determination, the result suggests that significant differential diffusion of T and S may indeed be a reality in the ocean.

5. Discussion and Conclusions:

At the present time, the conditions under which differential diffusion will produce significant effects in stratified aqueous flows cannot be regarded as well known. The conceptual picture considered in Section 1, in which scalar variance produced by stirring in the large eddies of a turbulent flow is subsequently strained to scalar dissipation scales in a time which depends upon scalar Schmidt number, might suggest that significant differential diffusion would arise only in low Re and/or intermittent turbulence, where fluid parcels could return to their original positions before an elapsed time large enough to complete scalar transfers. However there is evidence of the effects of differential diffusion in the continuously-forced turbulence of laboratory grid-stirring experiments, in the presumed quasi-steady turbulence measured in the ocean by Nash and Moum (2001), as well as in some high Re laboratory flows. Perhaps a more fundamental requirement is the existence in the scalar field of coherent structures such as those first revealed in a laboratory mixing layer by the classic shadowgraph photos of Brown and Roshko (1974). Broadwell and Mungal (1991) conclude that the sum of laboratory evidence (from both shear layers and jets) is that such large-scale coherent structures exist in all turbulent flows which have Reynolds numbers beyond some critical value. For flows in which such large-scale structures exist, Broadwell and Breidenthal (1982) formulated a simple two-stage Lagrangian model of mixing. In the first stage, the scalar is swept into "braid" regions between individual large eddy structures and strained from that scale (ℓ) down to the Kolmogorov viscous scale $\lambda_k = (\nu^3/\epsilon)^{1/4}$ by an inviscid cascade process which takes time $t_k \sim \ell/u$, where u is the large eddy velocity scale. The second stage occurs once λ_k is reached, when the scalar is assumed to diffuse (mix) instantaneously. Using the scale relation $\epsilon \sim u^3/\ell$,

this instant-diffusion assumption is seen to hold provided that the time t_λ required for diffusion across λ_k ,

$$t_\lambda \sim \frac{\lambda_k^2}{D_s} \sim \frac{\lambda}{u} \frac{Sc}{Re^{1/2}} \sim t_k \frac{Sc}{Re^{1/2}} \quad (1)$$

is negligible relative to t_k . However (1) suggests that in certain cases, ie for scalars with large Sc in flows of moderate to low Re , it will be necessary to modify this simple model to account for the additional time required to strain the scalar from λ_k to its dissipation scale $\lambda_s = \lambda_k Sc^{-1/2}$. For this more general case, Rehmann (1995) has estimated T_M , the total time required to strain and mix scalars, relative to the turbulence decay time T_D . His conceptual model is similar to that described earlier, ie that little mixing should occur when $T_M \gg T_D$ since a parcel displaced by the turbulence will be returned to or near to its original position by decay of the overturning eddy before there is time for significant transfer of scalar variance to its appropriate dissipation scale; this limit clearly predicts differential diffusion of scalars with different Sc . In contrast, when $T_M \ll T_D$, there is ample time for scalar variance to be transferred to small scales, mixing should be largely complete by the time the turbulence itself has decayed, and differential diffusion is absent. An added complication is that while most of the laboratory examples of differential diffusion involve passive scalars, hence inertial scaling of velocity time scales, the important oceanic scalars are both potentially active; ie variations of T and S affect the density of fluid parcels, and thus may modify the dynamics of the turbulence itself. Rehmann (1995) further postulates possible modifications of T_D , the turbulent decay time scale, associated with varying degrees of mean stratification, and uses these to predict different mixing regimes, dependent upon Re , Sc , and Richardson number Ri . In separate dimensional analyses focussed on the case of a thin stratified interface, Breidenthal (1992) predicts other regimes within this same function space. While both analyses predict regimes where differential diffusion

is to be expected, the results have not yet been critically tested in comparison with laboratory measurements, or with each other. An additional challenge will be to relate these (or other) predictions to oceanographically relevant situations and measurable variables.

If differential diffusion were to prove a significant process in a large part of the stratified ocean, it would require substantial re-evaluation of some of our present techniques for “measuring” (in fact estimating) diapycnal diffusion of density. If differential diffusion is important, the turbulent diffusivity $K_T \equiv \chi_T (T_z)^{-2}$ estimated from normalized T dissipation rate by the method of Osborn and Cox (1972) may represent a diffusivity K_p characteristic of density, but may equally well be totally unrelated to K_p , depending upon the relative contributions of T and S to the background density stratification. In the face of differential diffusion, it is only when $R_p \gg 1$, so that T dominates density, that $K_T \sim K_p$. If instead $R_p < 1$, as is the case in most coastal oceans, the North Pacific subarctic gyre, and parts of the Arctic and Antarctic Oceans, the temperature microscale measurement of K_T yields at most an upper bound on K_p . The true value of K_p , dominated by the less efficient transfer of salt, may be much smaller. An alternate technique is that of purposeful tracer releases (Ledwell et al. 1991; 1993) in which a conservative tracer is released on a density surface and its vertical spread, measured as a function of time, is used to estimate K_p . The considerable expense of this technique has been justified by the assumption that it yields a time-integrated measure of diapycnal density diffusion which is more accurate than that supplied by sporadic microscale measurements. However sulphur hexafluoride (SF_6), the conservative tracer used in most ocean releases, has a molecular diffusivity dependent on temperature (King and Saltzman 1995), so that the Schmidt number for SF_6 is near that of salt ($Sc_S \sim 600-700$) only at high temperatures ($T > 25^\circ C$). At lower temperatures, the Schmidt number for SF_6 increases, reaching a value 2-3 times that of S at $T \sim 10^\circ C$. Thus within large areas of the ocean, the diapycnal diffusion of SF_6 may not be that of either T or S, if differential diffusion is an important process. Even for temperatures at

which this measurement may be expected to yield the turbulent diffusivity of salt, in the presence of differential diffusion this diffusivity estimate may again be only loosely related to that for density.

This note has (i) reviewed irrefutable laboratory evidence for the existence of the process of differential diffusion, (ii) suggested that differential diffusion is likely to produce significant effects over parameter ranges which are typical of large volumes of the ocean, and (iii) provided examples of possible effects of differential diffusion in some ocean observations. Given the importance of differential diffusion to the correct interpretation of diffusivity estimates from both standard microscale measurements and tracer release experiments, as well as the development of appropriate parameterizations of vertical mixing of scalars in any numerical model of the ocean, it seems essential to make the necessary efforts to better understand this process in the oceanic context.

REFERENCES:

Altman, D. B., and A. E. Gargett, 1990. Differential property transport due to incomplete mixing in a stratified fluid. *Stratified Flows*, E. J. List and G. H. Jirka, Eds., American Society of Civil Engineers, New York, 454-460.

Bilger, R. W. 1989. Turbulent diffusion flames. *Ann. Rev. Fluid Mech.*, 21, 101-135.

Breidenthal, R.E. 1992: Entrainment at thin interfaces: the effects of Schmidt, Richardson, and Reynolds numbers. *Phys. Fluids*, A4(10), p. 2141-2144.

Broadwell, J. E. and R. E. Breidenthal. 1982. A simple model of mixing and chemical reaction in a turbulent shear layer. *J. Fluid Mech.*, 125, 397- 410.

Broadwell, J. E. and M. G. Mungal. 1991. Large-scale structures and molecular mixing. *Phys. Fluids A*, 3, 1193-1206.

Brown, G. L. and A. Roshko. 1974. On density effects and large structure in turbulent mixing layers. *J. Fluid Mech.* 64(4), 775-816.

Bryan, F. 1987: On the parameter sensitivity of primitive equation ocean general circulation models. *J. Phys. Oceanogr.*, 17, 970-985.

Fernando, H. J. S. 1991: Turbulent mixing in stratified fluids. *Ann. Rev. Fluid Mech.*, 23, 455-494.

Gargett, A. E. 1988: Reynolds number effects on turbulence in the presence of stable stratification. *Small-Scale Turbulence and Mixing in the Ocean*. Eds. J.C.J. Nihoul and B.M. Jamart. Elsevier Science Publishers, 517-528.

Gargett, A.E. 1997: "Theories" and techniques for observing turbulence in the ocean euphotic zone. **In** *Lecture Notes on Plankton and Turbulence*, eds. C. Marrasé., E.Saiz and J.M.Redondo, *Scientia Marina*, **61**(Suppl), 25-45.

Kerstein, A. R. 1990. Linear-eddy modelling of turbulent transport. Part 3. Mixing and differential molecular diffusion in round jets. *J. Fluid Mech.*, 216, 411-435.

King, D. B. and E. S. Saltzman. 1995. Measurement of the diffusion coefficient of SF₆ in water. *J. Geophys. Res.*, 100, 7083-7088.

Komori, S. and K. Nagata 1996. Effects of molecular diffusivities on counter-gradient scalar and momentum transfer in strongly stable stratification. *J. Fluid Mech.*, 326, 205-237.

Ledwell, J.R. and A.J. Watson. 1991: The Santa Monica Basin tracer experiment: a study of diapycnal and isopycnal mixing. *J. Geophys. Res.*, **96**(C5), 8695-8718.

Ledwell, J.R., A.J. Watson and C.S. Law. 1993: Evidence for slow mixing across the pycnocline from an open-ocean tracer-release experiment. *Nature*, 364, 701-703.

Merryfield, W. J., G. Holloway and A. E. Gargett. 1998a. Differential vertical transport of heat and salt by weak stratified turbulence. *Geophys. Res. Letters*, 25, 2773-2776.

Merryfield, W. J. 2001. Intrusions in doubly-stable Arctic waters: evidence for differential mixing? *J. Phys. Oceanogr.*, submitted.

Osborn, T.R. and C.S. Cox. 1972: Oceanic fine structure. *Geophys. Fluid Dyn.*, 3, 321-345.

Padman, L. and T.M. Dillon. 1987: Vertical heat fluxes through the Beaufort Sea thermohaline staircase. *J. Geophys. Res.*, 92(C10), 10799-10806.

Rehmann, C.R. 1995. Effects of stratification and molecular diffusivity on the mixing efficiency of decaying grid turbulence. PhD Thesis, Stanford University.

Rudels, B., E. P. Jones, L. G. Anderson and G. Kattner 1994. On the intermediate depth waters of the Arctic Ocean. in *The Role of the Polar Oceans in Shaping Global Climate*, ed. O. M. Johannessen, R. D. Meunch and J. E. Overlans, AGU, Washington, 33-46.

Saylor, J. R. 1993. Differential diffusion in turbulent and oscillatory, non-turbulent, water flows. Ph.D. Thesis, Yale University.

Saylor, J. R. 1997. Measurements of differential diffusion in a liquid-filled lung model. *Exp. Fluids*, 23, pp. 498-503.

Saylor, J. R. and K. R. Sreenivasan 1997. Differential diffusion in low Reynolds number water jets. *Phys. Fluids*, 10(5), 1135–1146.

Turner, J. S. 1968. The influence of molecular diffusivity on turbulent entrainment across a density interface. *J. Fluid Mech.*, 33, 639-656.

Walsh, D. and B. Ruddick 1998. Nonlinear equilibration of thermohaline intrusions. *J. Phys. Oceanogr.*, 28, 1043-1070.

Yeung, P. K. and S. B. Pope 1993. Differential diffusion of passive scalars in isotropic turbulence. *Phys. Fluids A*, 5(10), 2467-2478.